

# RSC Advances



This is an *Accepted Manuscript*, which has been through the Royal Society of Chemistry peer review process and has been accepted for publication.

*Accepted Manuscripts* are published online shortly after acceptance, before technical editing, formatting and proof reading. Using this free service, authors can make their results available to the community, in citable form, before we publish the edited article. This *Accepted Manuscript* will be replaced by the edited, formatted and paginated article as soon as this is available.

You can find more information about *Accepted Manuscripts* in the [Information for Authors](#).

Please note that technical editing may introduce minor changes to the text and/or graphics, which may alter content. The journal's standard [Terms & Conditions](#) and the [Ethical guidelines](#) still apply. In no event shall the Royal Society of Chemistry be held responsible for any errors or omissions in this *Accepted Manuscript* or any consequences arising from the use of any information it contains.



Journal Name

ARTICLE

## The effect of architecture/composition on the pH sensitive micelle properties and in vivo study of curcumin-loaded micelles containing sulfobetaines

Received 00th January 20xx,  
Accepted 00th January 20xx

DOI: 10.1039/x0xx00000x

www.rsc.org/

Zhengzhong Wu,<sup>a</sup> Mengtan Cai,<sup>a</sup> Xiaoxiong Xie,<sup>a</sup> Liu He,<sup>a</sup> Lei Huang,<sup>a</sup> Yuanwei Chen<sup>\*a</sup> and Xianglin Luo<sup>\*ab</sup>

Polymeric architecture greatly influences the properties of the polymer drug carriers. In this study, copolymers poly( $\epsilon$ -caprolactone)-*b*-poly(N,N-diethylaminoethyl methacrylate)-*r*-poly(N-(3-sulfopropyl)-N-methacryloxyethyl-N,N-diethylammoniumbetaine) with linear (L-PCL-PDEASB) and four-armed star-shape (4s-PCL-PDEASB) were designed and prepared to explore the relationship between the architecture/composition and the micelle properties. The structure of these copolymers were characterized by nuclear magnetic resonance (NMR), Fourier transform infrared (FTIR), elemental analysis, gel permeation chromatograph (GPC), differential scanning calorimetry (DSC), and water contact angle (WCA). The results showed that the copolymer composition/structure affect their thermal properties, hydrophilicity, micelle properties, pH sensitivity and drug releasing performance. In cytotoxicity experiment the micelles of star-shaped copolymer displayed lower cell toxicity than those of the linear copolymer with the same composition. The drug release rate of the curcumin-loaded micelles was related to sulfobetaine units and was much different for different copolymer micelles. The curcumin-loaded micelles of star-shaped copolymer prolonged the retention time of curcumin in blood circulation in pharmacokinetic experiment and accumulated more in tumor site than the free curcumin in breast carcinoma bearing mice in drug distribution experiment. The tissue section images illustrated that the curcumin-loaded micelles could reduce curcumin damage to liver and lung. Therefore, the pH sensitive micelles of star-shaped copolymer containing sulfobetaines with suitable composition are promising carriers.

### Introduction

In the past decades, biodegradable micelles have been the most promising drug delivery system (DDS) for cancer therapy because of their enhanced drug loading capability, prolonged blood circulation time, accumulation at tumor tissues by EPR effect and feasible functionality through molecular design.<sup>1-4</sup> However, most of the micelles for tumor drug delivery often exhibit inefficient accumulation and insufficient drug release at tumor tissues or in tumor cells just passively through EPR effect. To solve this problem, efforts of researchers have been much concentrated on developing micelle delivery system with environment responsive properties, especially with pH sensitivity based on the instinct of tumors. It has been reported that the pH of extracellular matrix (ECM) in normal tissue and of blood is usually at pH 7.2–7.4 while the mean pH in various solid tumors is 7.06,<sup>5-8</sup> with a range of 5.7–7.8, pH of endosome is 5.0~6.0, and pH of lysosome is even lower, about

4.0~5.0. Based on the pH differences between ECM of tumors and normal tissue/blood or between ECM and inside of tumors, pH sensitive micelles for enhanced accumulation and drug release at tumor site might be designed.<sup>1,7-11</sup> The approaches to obtain pH sensitive micelles are to use the copolymers containing acid-labile chemical bonds or “ionizable” chemical groups, such as poly(acrylic acid), poly(histidine), poly(2-(diethylamino)ethyl methacrylate) (PDEA). With a pH around 7.2, PDEA is protonated when it is exposed at slightly acidic condition, thus usually used as a pH sensitive micelle component to respond the pH change from blood to tumor tissues.<sup>12</sup> Till now, PDEA has been included in many drug delivery systems to provide pH response property for micelles.<sup>9,12-16</sup>

Due to the insolubility of PDEA at pH above 7.2, poly(ethylene glycol) (PEG) in most drug delivery systems containing PDEA is usually used as the hydrophilic part of the drug delivery carriers. PEG has water solubility, biocompatibility and stealth property. However, the shielding effect of PEG shell is unfavorable for cellular uptake, thus, many studies focus on exploring new hydrophilic polymers for DDS.<sup>7</sup> Recently, polymers containing zwitterions such as sulfobetaine groups have aroused great attentions for their good water solubility and excellent biocompatibility featured

<sup>a</sup> College of Polymer Science and Engineering, Sichuan University, Chengdu, 610065, China. E-mail: luoxl\_scu@126.com; Fax: +86 28 85466166; Tel: +86 28 85466166.

<sup>b</sup> State Key Laboratory of Polymer Materials Engineering, Sichuan University, Chengdu, 610065, China. E-mail: luoxl\_scu@126.com; Fax: +86 28 85466166; Tel: +86 28 85466166.

by non-fouling and protein-resistance properties.<sup>17-20</sup> Recently, several studies have focused on introducing sulfobetaine into DDSs.<sup>6,13,15,21</sup> In our previous studies, we designed and synthesized copolymers composed with biodegradable PCL, pH sensitive PDEA and sulfobetaine groups.<sup>13</sup> The micelles of the copolymers showed good drug loading capability, good biocompatibility and enhanced cell uptake. For the micelles, PDEA is as the pH-sensitive part and introduced zwitterionic sulfobetaine is as a part to enhance hydrophilicity/protein adsorption-resistance and to influence the local environment for PDEA. However, for the moment, the effect of the copolymer architecture and composition on the pH sensitive micelles containing sulfobetaines is unknown. It has been widely reported that the properties of micellar DDS are greatly influenced by the architecture of the self-assembling polymers. In addition, the pH-sensitivity of pH sensitive micelles may be influenced by other polymers such as PEG connected with PDEA.<sup>22</sup> Furthermore, although the pH sensitive micelles containing sulfobetaines showed good ability for cellular uptake,<sup>23</sup> there is only a few studies on the in vivo properties of this kind micelles up to now.

To better understand the relationship between the architecture of copolymers and properties of micelles, and to optimize the designed pH sensitive micellar DDS, in this study three copolymers with linear (L-PCL-PDEASB) and four-armed star-shape (4s-PCL-PDEASB) were prepared. The properties such as crystallinity, hydrophilicity, micellization behavior for the copolymers and drug-loading/releasing properties, pH sensitivity and cell toxicity in vitro for the copolymer micelles were studied and compared. Furthermore, the star-shaped copolymer micelles were used as drug carriers and The widely studied model drug curcumin was used as model drug for in vivo pharmacokinetics, drug distribution and histopathology experiments, since its effect on inflammation, anti-oxidation, anti-rheumatoid, and tumor growth inhibition etc and its hydrophobicity is suitable to be encapsulated into micelle.

## Materials and Methods

### Materials

N, N-diethylaminoethyl methacrylate (DEA) (Aldrich, USA) and  $\epsilon$ -caprolactone (CL) (New Jersey, USA) were dried by calcium hydride ( $\text{CaH}_2$ ) and distilled under reduced pressure. Toluene and tetrahydrofuran (THF) (Chengdu Kelong Chemicals Ltd., China) were dried by refluxing over sodium and distilled before used. Triethylamine (TEA) was dried over calcium hydride ( $\text{CaH}_2$ ) and distilled. Stannous octanoate ( $\text{Sn}(\text{Oct})_2$ , 95%), 2-bromoisobutyl bromide (98%), copper (I) bromide (CuBr, 99%), 2,2-bipyridine (bpy), pentaerythritol, 3-[4, 5-dimethylthiazol-2-yl]-2, 5-diphenyltetrazolium bromide (MTT) were purchased from sigma (USA) and used as received. 1,3-propanesultone (PS) was supplied by Acros (Belgium) and used as received. Heparin sodium offered by Aladdin (USA) and used as received. All the reagents and solvent without specific description were purchase from Chengdu Kelong

Chemicals Ltd., China. All the other reagents and solvents were of analytical grade and used without further purification.

### Synthesis of copolymers

The copolymers were prepared according to our previous study.<sup>13</sup> Using laurinol or pentaerythritol as the initiator, linear PCL or four-armed PCL was obtained by ring opening polymerization and then 2-bromo-2-methylpropanoyl bromide was used to react with PCL to generate the maroinitiator, which was used to initiate the polymerization of DEA through ATRP. At last, part of DEA groups were converted to sulfobetaine by reaction with PS.

### Characterization of the polymer

<sup>1</sup>H NMR spectra were recorded on a Unity Inova 400 spectrometer operating at 400 MHz. The molecular weight and polydispersity of the copolymers were determined by a Waters 1515 gel permeation chromatograph instrument system. The measurements were performed using THF as the eluent at a flow rate of 1.0 mL/min at 30 °C and a series of narrow polystyrene standards for the calibration of the columns. Element analysis was performed on an elemental analyzer (Euro EA 3000) with the samples being around 0.8 mg. Fourier-transform infrared spectra (FT-IR) were recorded on a Nicolet 560 (Nicol, American) spectrometer at wavelengths ranging from 500  $\text{cm}^{-1}$  to 4000  $\text{cm}^{-1}$  over 32 scans. The DSC analysis was carried out with a TA instrument under a nitrogen flow (10 mL/min). All samples were heated firstly from 40 to 100 °C at 10 °C/min and held for 5 min to erase the thermal history, then cooled to -80 °C at the rate of 10 °C/min, and finally heated to 100 °C at the heating rate of 10 °C/min. Water contact angle was measured using Drogmeter 100 equipment (Maist Vision, Ningbo, China) by the sessile drop technique. Specimen for contact angle observation was prepared by dropping 50  $\mu\text{L}$  of polymer solution (10 mg/mL) in volatile solvent (THF/Methanol, v/v=1:1) onto the glass wafer for twice, and then the sample was naturally dried at room temperature. Before measuring, the sample was again dried overnight in a vacuum oven at 35 °C.

### Preparation of the micelles

The conclusions section should come in this section at the end of the article, before the acknowledgements Micelles were prepared by solvent evaporation method. Briefly, the copolymers or the mixture of copolymers and curcumin with a weight ratio of 5:1 were firstly dissolved in a mixed solvent of THF/methanol (v/v=1:1) to give a stock polymer solution of 5 mg/mL, and then 2 mL of the stock polymer solution was added dropwise into 10 mL of ultrapure water at a speed of 100  $\mu\text{L}/\text{min}$  under vigorous stirring, followed by solvent evaporation using a rotary vacuum evaporator for 10 min to remove residual solvent. And then the micelle solution was filtered by 0.45  $\mu\text{m}$  filter. Dynamic light scattering (DLS)

measurements were performed to determine the micellar size and distribution using a Malvern Zetasizer Nano Series equipped with DTS software and operating a 4 mW He–Ne laser at 633 nm. Analysis was performed at an angle of 90° and a constant temperature of 25 °C.

Drug loading content (DLC) and drug loading efficiency (DLE) was determined by ultraviolet spectroscopy and calculated by the following equations:

$$\text{DLC} = (\text{Mass of the drug encapsulated in the micelle}) / (\text{Mass of the micelle}) \times 100\% \quad (1)$$

$$\text{DLE} = (\text{Mass of the drug encapsulated in the micelle}) / (\text{Mass of drug used for micelle preparation}) \times 100\% \quad (2)$$

### Measurement of the critical micelle concentration (CMC)

The critical micelle concentration (CMC) for each copolymer in water was estimated by using pyrene as a hydrophobic fluorescence probe. Samples of micellar solution with concentrations ranging from  $5 \times 10^{-7}$  to  $1 \text{ g L}^{-1}$  were prepared and then left to equilibrate with a constant pyrene concentration of  $6 \times 10^{-7} \text{ M}$  for 48 h. Fluorescence spectra of pyrene were recorded with a fluorescence spectrophotometer (F-7000, Hitachi Co., Ltd) at room temperature. Emission was carried out at 395 nm, and excitation spectra were recorded ranging from 240 to 360 nm. Both excitation and emission slit widths were 2 nm. The CMC was determined from the intersection of two straight lines (the horizontal line with almost constant value of the ratio  $I_{336}/I_{333}$  and the vertical line with a steady increase in the ratio value) on the graph of the fluorescence intensity ratio  $I_{336}/I_{333}$  versus log polymer concentration.

### Basic titration

The titration curves of these copolymers were obtained by an acid–base titration method. Blank micelles of certain copolymer were prepared with ultrapure water (50 mL, 1 mg/mL). The pH of the solution was adjusted to around 2.0 by addition of HCL aqueous solution (1 M). The increase of pH was recorded a pH meter (Starter 3C, Ohaus, USA), during the process of slowly adding NaOH aqueous solution (0.1M).

### The Morphology of Micelles

The morphology of these micelles in pH 5.0 and pH 7.4 was observed by SEM. The micelle solution was diluted to 0.004 mg/mL, and then 20  $\mu\text{L}$  diluted solution was added onto a glass slide and frozen drying. The glass slide with the micelles was observed by SEM.

### In vitro drug release

The drug release of curcumin loaded in micelles in different pH was investigated by dialysis method. Briefly, each sample of curcumin-loaded micelles was placed into a dialysis membrane bag (Mw=3500). The bag was sealed and immersed 300 mL PBS (0.01 M, pH = 7.4 or pH = 5.0.), in a shaking bed with the shaking rate of 100 rpm at 37 °C. PBS was refreshed for per 2 h in the beginning and for per 4 h after 6 h. At different predetermined time intervals, 200  $\mu\text{L}$  of the micelle solution was taken out and residual content of curcumin in the micelles was analysed by ultraviolet spectroscopy.

### In vitro cytotoxicity

In vitro cytotoxicity of the micelles was evaluated by 3-(4,5-dimethylthiazol-2-yl)-2,5-diphenyltetrazoliumbromide (MTT) assay. LO2 cells were obtained from Huaxi Medical Research Center of Sichuan University. The cells were seeded in 96-well plates at around 2,000 cells per well in RPMI 1640 culture medium containing 10% fetal bovine serum, supplemented with 40~50 U/mL penicillin and 50 U/mL streptomycin, and incubated at 37 °C in 5% CO<sub>2</sub> atmosphere for 24 h. Then the culture medium was replaced with fresh culture medium containing blank micelles with different concentration. After 24 h or 72 h, 20  $\mu\text{L}$  of MTT solution (5 mg/mL) was added to each well. After 4 h of incubation at 37 °C, the MTT solution was replaced with 150  $\mu\text{L}$ /well dimethyl sulfoxide (DMSO), followed by 10 min shaking. The optical densities (OD) of each well were determined with a microplate reader at a wavelength of 490 nm. Cells cultured without micelles were set as the blank control. The cell viability was calculated according to the following formula:

$$\text{Cell viability}(\%) = \text{ODt} / \text{ODb} \times 100\% \quad (3)$$

Where ODt and ODb are the OD values of surviving cells treated with sample solution and the OD values of blank control, respectively. Each experiment was repeated five times for each sample.

### In vivo pharmacokinetics

SD mice weights 200 to 220 g were purchased from Experimental Animal Center of Sichuan University (Chengdu, China). All animal experiments complied with the requirements of the institute's animal care and use committee. Prior to the experiment, the mice were fasted for 12 hours but were allowed free access to water. Free curcumin was dissolved in a mixture solution (DMA, PEG400, and 5% dextrose solution with 3 : 9 : 8 volumetric ratio) to form a free curcumin solution (approximately 2 mg/mL) for injection. The curcumin-loaded micelles have DLC about 20%, absolutely curcumin concentration approximately 2mg/mL. Free curcumin solution and curcumin-loaded micelles were administered intravenously tail vein with a dosage of 10 mg/kg body weight, respectively (n=6 for each group). At different time points (0.033 h, 0.1 h, 0.3 h, 0.5 h, 1 h, 2 h, 4 h, 8 h, 24 h post-injection), 400  $\mu\text{L}$  blood was collected in a heparinized tube through tail cutting. Then, blood samples were centrifuged immediately at 4°C, 5000 rpm/min for 10

min to obtain plasma. 150  $\mu\text{L}$  plasma was added with 50  $\mu\text{L}$  citrate buffer solution, vortexed for 3 min. The solution was diluted to 1.5 mL by adding methanol, whirled for 10 min and centrifuged at 4  $^{\circ}\text{C}$ , 10000 rpm/min for 10 min. 200  $\mu\text{L}$  supernatant was added to 96 well plate and the fluorescence was determined at excitation/emission of 420/540 nm using a fluorescence ELISA (Thermo Scientific Varioskan Flash, USA). Curcumin concentration in blood was calculated by standard curve which was generated by the addition of free curcumin to methanol and step diluted from 1000 ng/mL to 20 ng/mL. Finally, Non-compartmental pharmacokinetic analysis was done using the Drug and Statistics (DAS) software (version 2.1.1, Mathematical Pharmacology Professional Committee of China).

### Biodistribution

BALB/c mice bearing breast carcinoma (weight 18-22 g, tumour 150-300  $\text{mm}^3$ ) were randomly allocated to three groups and were fasted for 12h before experiment. Curcumin solution (2mg/mL), curcumin-loaded micelles of 4s-PCL<sub>20</sub>PDEA<sub>15</sub>SB<sub>5</sub> (DLC about 20%, absolutely curcumin concentration approximately 2 mg/mL) and normal saline were injected into these mice via tail vein at a dose of 10 mg/kg body weight, respectively (n=5, 5, 2). At 6 h post-injection, the mice were sacrificed, and their major organs (heart, liver, spleen, lung and kidney) and tumor tissue were harvested from the mice. After swashing with normal saline and sucking water by filter papers, these tissues/organs for each group were cut with scissors into two parts, one part for biodistribution study, the other for staining pathologic sections. The tissues used for biodistribution study were weighed firstly and then homogenized using FJ-200 Kinematica (Shanghai specimen model factory, China), and were followed with 3 min eddy after adding 500  $\mu\text{L}$  citric acid-sodium citrate buffer solution (PH=3.0). These mixtures were diluted to 3 mL using methanol and were whirled for 10 min, then centrifuged at 4 $^{\circ}\text{C}$ , 10000 rpm/min for 10 min. Curcumin concentration in organs was obtained using the same method mentioned above.

### Histopathology

The tissues used for staining pathologic sections were immersed immediately in fixative (AAF solution, the mixture of 85 mL 95%-100% alcohol, 5 mL glacial acetic acid, 10 mL concentrated formaldehyde) for 24 h. The tissues were cut into 5 mm  $\times$  10 mm  $\times$  5 mm pieces, and embedded in paraffin after gradient elution using ethanol. Slices 5 $\mu\text{m}$  thick were prepared and stained with haematoxylin and eosin (H&E). Finally, the pathological changes of the organs were observed under light microscope.

### Result and discussion

### Synthesis of copolymers

In this study, pH sensitive copolymers with linear and four-armed star-shape, poly( $\epsilon$ -caprolactone)-b-poly(N,N-diethylaminoethylmethacrylate)-r-poly(N-(3-sulfopropyl)-N-methacryloxyethyl-N,N-diethylammoniumbetaine) (PCL-PDEASB), were designed and prepared by the combination of ring opening polymerization (ROP) and atom radical transfer polymerization (ATRP) and final sulfonation. Similar operation process and technological details were reported in our previous work.<sup>13</sup> For linear copolymers, the initiator used in ROP of  $\epsilon$ -caprolactone was laurinol, while pentaerythritol was used as the initiator for four-armed star shape copolymer. The structure of the copolymers was confirmed by FT-IR,  $^1\text{H}$  NMR, and element analysis.

Figure 1 showed  $^1\text{H}$  NMR spectra of linear and four-armed star shape copolymers before and after sulfonation. In the spectra of L-PCL<sub>20</sub>PDEA<sub>20</sub> and 4s-PCL<sub>20</sub>PDEA<sub>20</sub>, there were characteristic resonances of PCL at 1.38 ppm, 1.65 ppm, 2.31 ppm, and 4.05 ppm. In addition, typical methylene proton signals of PDEA copolymer were observed at 2.58 ppm (–N–CH<sub>2</sub>CH<sub>3</sub>), 2.64 ppm (–NCH<sub>2</sub>CH<sub>2</sub>OOC–, methylene proton neighboring to the nitrogen atom,) and 3.99 ppm (–NCH<sub>2</sub>CH<sub>2</sub>OOC–, methylene proton neighboring to ester group). The new peaks (r, s, w and t) appeared in the  $^1\text{H}$  NMR spectra of PCL-PDEASB copolymers were assigned to sulfobetaine groups, and remained characteristic peaks of DEA indicated part sulfonation of the tertiary amines. The unit number of sulfobetaines was determined by the integrating ratio of peak r from sulfobetaine and peak c from the PCL block.

**Figure 1.**  $^1\text{H}$  NMR spectra for (1) L-PCL<sub>20</sub>PDEA<sub>20</sub> in CDCl<sub>3</sub>; (2) 4sPCL<sub>20</sub>PDEA<sub>20</sub> in CDCl<sub>3</sub>; (3) L-PCL<sub>20</sub>PDEA<sub>15</sub>SB<sub>5</sub> in the mixture of CDCl<sub>3</sub> and CD<sub>3</sub>OD; (4) 4sPCL<sub>20</sub>PDEA<sub>15</sub>SB<sub>5</sub> in the mixture of CDCl<sub>3</sub> and CD<sub>3</sub>OD.

FT-IR was used to qualitatively analyze the obtained copolymer (Figure S1). The new peak around 1154  $\text{cm}^{-1}$  in the curve for L-PCL<sub>20</sub>PDEA<sub>20</sub> compared with L-PCL<sub>20</sub> was attributed to the vibration of C-N of the tertiary amine in PDEA block. After sulfonation of L-PCL<sub>20</sub>PDEA<sub>20</sub>, new peaks appeared 1641  $\text{cm}^{-1}$  assigned to the vibration of C-N<sup>+</sup>, meanwhile, the vibration peak of S-O and S=O appeared at 1211  $\text{cm}^{-1}$  and at 1038  $\text{cm}^{-1}$ , respectively. Moreover, these peaks assigned with sulfobetaine group became stronger significantly as the content of sulfobetaine increased. Similar characteristic peaks were found with the FT-IR in four-armed copolymer.

Element analysis was performed to obtain the mass ratio of sulfur and nitrogen, which also revealed the unit number of sulfobetaines. The unit numbers of sulfobetaine groups calculated from  $^1\text{H}$  NMR and from element analysis were close. The compositions data for the copolymer were summarized in Table 1. Therefore, the actual composition/structure of the copolymers coincided with designed composition/structures.

In Table 1 the thermodynamic data of the synthesized copolymers were also listed, since the crystallization properties of polymers influence their degrading behavior,<sup>24</sup>

drug loading capability<sup>25</sup> and drug release behavior<sup>6</sup>. The melting curve and cooling curve were shown in Figure S2. For linear or four-armed copolymers, introduction of PDEA to PCL and introduction of ulfobetaine to PCL-PDEA reduced the degree of crystallization. PDEA blocks limited the mobility of PCL segments, which resulted decrease of crystalline capability of PCL. Moreover, four-armed copolymer showed lower melting temperature and crystallization degree than that of the linear copolymer with the same composition. This may be attributed to the star-shaped structure, which limits the polymer chains incorporating into the crystallites.<sup>24,26</sup>

### Hydrophilicity of the copolymers

Appropriate hydrophilicity for amphiphilic copolymers is important during forming micelles. Hydrophilicity of the prepared copolymers was investigated via water contact angle measurement, as shown in Figure 2. The water contact angles of these three copolymers were less than 80° due to the existence of hydrophilic sulfobetaines and decreased with time increasing for each sample owing to immigration of sulfobetaines. The water contact angle of L-PCL<sub>20</sub>PDEA<sub>10</sub>SB<sub>10</sub> was less than that of L-PCL<sub>20</sub>PDEA<sub>15</sub>SB<sub>5</sub>, meaning that increasing sulfobetaine content brings stronger hydrophilicity.

Furthermore, reduction of water contact angle for L-PCL<sub>20</sub>PDEA<sub>10</sub>SB<sub>10</sub> was more obvious than that of L-PCL<sub>20</sub>PDEA<sub>15</sub>SB<sub>5</sub> during the same period of time as a result of increasing hydrophilicity of the copolymer surface.<sup>15,27</sup> On the other hand, although linear L-PCL<sub>20</sub>PDEA<sub>15</sub>SB<sub>5</sub> and star-shaped 4s-PCL<sub>20</sub>PDEA<sub>15</sub>SB<sub>5</sub> had same composition, the contact angles of copolymers for them were much different and decreased differently during the same period of time. It was attributed to limite movement of polymer chains in star-shaped copolymer. Due to limite movement of polymer chains in 4s-PCL<sub>20</sub>PDEA<sub>15</sub>SB<sub>5</sub>, the migration of the hydrophilic chains reduced, and less sulfobetaine groups migrated to the surface of the films, thus the water contact angle of star-shaped copolymers was higher than that of linear copolymer.<sup>27</sup>

**Figure 2.** (A) The water contact angles of the copolymers and (B) the photographs of water contact angle of the copolymers at 3s and 60s.

### Properties of the blank micelles and curcumin loaded micelles

Generally, amphiphilic copolymers can self-assemble into micelles in water with lipophilic core and hydrophilic shell.<sup>28</sup> The copolymers bearing PCL and sulfobetaine groups can easily form micelles, with sulfobetaine as the shell and PCL segment as the core in aqueous solution. The copolymers obtained in this work could form micelles as other amphiphilic copolymers. Their low CMC values, around 10<sup>-3</sup> mg/mL, proved micelle ability were shown in Table 2. CMC values of two linear copolymers weresimilar and decreased a bit with the DEA group content increasing, while CMC value for the four-armed copolymer was much lower than that of both

linear copolymers. As we all knew, DEA groups are mostly deprotonated at neutral condition, more DEA groups in the copolymer result in higher content of hydrophobic part. Consequently, the copolymer having more DEA groups had lower CMC. As to 4s-PCL<sub>20</sub>PDEA<sub>15</sub>SB<sub>5</sub> having the lowest CMC, It's because many arms exist in unimer state of a star-shape copolymer. And when the copolymer resembled its micellar state, formation of micelles was easier.<sup>6</sup>

Micelle sizes are important for anti-tumor drug delivery, because sizes are directly relevant to whether micelles can be used as anti-tumor drug carriers. The mean diameters of the blank micelles were around 60-70 nm, meanwhile, curcumin-loaded micelles were 75-110 nm. And such micelle sizes are applicable as anti-tumor drug carriers, for micelles with size around 100 nm can effectively accumulate at the tumor site through enhanced permeability and retention effect (EPR).<sup>28</sup> No matter which blank and drug-loaded micelles, the mean diameters of two linear copolymers micelles decreased with the increasing of DEA groups. This is because more protonated DEA groups will result in electrostatic repulsion increase in the micelle shells, thus, leading to form smaller micelles. Furthermore, the four-armed copolymer micelles showed slightly larger sizes in comparison with its linear counterpart. The difference might be related to crystallization ability of core-formed parts. The four-armed copolymer could only form looser cores because 4s-PCL<sub>20</sub>PDEA<sub>15</sub>SB<sub>5</sub> had lower crystallization ability, as indicated in Table 1. Moreover, these drug-loaded micelles showed larger size when compared with their corresponding blank micelles, because curcumin was loaded into the core of these micelles.<sup>29</sup>

The particles with positive charges facilitate adhesion to cell membrane and thus favor endocytosis by cells. All the micelles in the work showed positive zeta-potential values around 40-60 mV. Thus, the micelles formed by pH-sensitive copolymer containing zwitterionic sulfobetaines would be favored for cellular endocytosis. L-PCL<sub>20</sub>PDEA<sub>15</sub>SB<sub>5</sub> micelles and 4s-PCL<sub>20</sub>PDEA<sub>15</sub>SB<sub>5</sub> micelles showed similar zeta-potentials because of their similar constitutional unit ratio, the micelle zeta-potential value was higher than that of L-PCL<sub>20</sub>PDEA<sub>10</sub>SB<sub>10</sub> micelles.

As for the drug-loaded micelles, zeta-potential values were all larger than that of their blank micelles. This may be caused by the phenolic hydroxyl group in curcumin which donated positive protons resulting in the protonation of PDEA.

In addition, drug loading content and drug loading efficiency of the drug-loaded micelles were measured. Hydrophobic curcumin was easily loaded into the PCL cores of amphiphilic PCL-copolymer micelles and high drug loading content could be achieved with these micelles.<sup>29,30</sup> As shown in Table 2, when copolymers were composed by PCL, PDEA and sulfobetaines

DLC and DLE for drug-loaded micelles were as high as other PCL-copolymer micelle's. DLC and DLE were more than 10% and over 50%, separately, which indicated that these drug-loaded micelles have the potential as effective drug delivery carriers.

### PH sensitivity

Many reports showed that PDEA-based copolymer micelles displayed pH sensitivity based on the protonation and deprotonation of DEA groups.<sup>11,13,15</sup> In this study, the pH sensitivity of PCL-PDEASB micelles was investigated. Acid–base titration of the micelles with a concentration of 1 mg mL<sup>-1</sup> was performed in comparison with pure water. As shown in Figure 3(A), pH value of pure water jumped up sharply from around 3 to about 10 with adding NaOH solution, while PCL-PDEASB micelles showed a pH buffering path which ranged from 5.5 to 7.0. Specifically, the buffering path was broad for L-PCL<sub>20</sub>PDEA<sub>15</sub>SB<sub>5</sub> and 4sPCL<sub>20</sub>PDEA<sub>15</sub>SB<sub>5</sub>, but was relatively narrow and abrupt for L-PCL<sub>20</sub>PDEA<sub>10</sub>SB<sub>10</sub>. This is due to the protonation of the PDEA, and the more DEA groups in the micelles there are, the stronger buffering of the micelles shows. Moreover, acidic titration for the micelle solution L-PCL<sub>20</sub>PDEA<sub>15</sub>SB<sub>5</sub> was carried out after its basic titration process. A similar titration curve was obtained, which indicated that the protonating and deprotonating of DEA groups were reversible, and thus the pH sensitivity of PCL-PDEASB micelles was reversible.

**Figure 3.** Titration curves of pure water, L-PCL–PDEASB micelles and 4s-PCL–PDEASB micelles with NaOH (left) and titration curves of L-PCL<sub>20</sub>PDEA<sub>15</sub>SB<sub>5</sub> micelles after its basic titration with acid (right).

Furthermore, SEM was employed to observe the morphology of the micelles at pH 7.4 and pH 5.0 (Figure 4). SEM images showed that the shapes of these micelles were spherical or sphere-like. The sizes of the micelles were about 102 nm, 87 nm and 89 nm at pH 7.4 for L-PCL<sub>20</sub>PDEA<sub>15</sub>SB<sub>5</sub>, L-PCL<sub>20</sub>PDEA<sub>10</sub>SB<sub>10</sub>, and 4sPCL<sub>20</sub>PDEA<sub>15</sub>SB<sub>5</sub>, respectively. And at pH 5.0 the sizes of all these micelles increased, were around 201 nm, 201 nm and 143 nm for L-PCL<sub>20</sub>PDEA<sub>15</sub>SB<sub>5</sub>, L-PCL<sub>20</sub>PDEA<sub>10</sub>SB<sub>10</sub>, and 4s-PCL<sub>20</sub>PDEA<sub>15</sub>SB<sub>5</sub> respectively. Size increase of pH sensitive micelles at acidic condition was observed in our previous study.<sup>13</sup> With pH decreasing from 7.4 to 5.0, many DEA groups were protonated and the electrostatic repulsion of positive charges of protonated DEA groups resulted in the expansion of the shell of these micelles, therefore, the micelle sizes increased.

**Figure 4.** Morphology of the different copolymer micelles at pH=7.4 (top) and pH=5.0 (bottom). A and A' for L-PCL<sub>20</sub>PDEA<sub>15</sub>SB<sub>5</sub>, B and B' for L-PCL<sub>20</sub>PDEA<sub>10</sub>SB<sub>10</sub>, C and C' for 4s-PCL<sub>20</sub>PDEA<sub>15</sub>SB<sub>5</sub>. (The bar means 100nm)

### In vitro drug release with different pH.

The drug release of the drug-loaded pH sensitive micelles containing sulfobetaines was performed under a physiological conditions (PBS, pH 7.4) and a slightly acidic environment (PBS, pH 5.0), the latter was to simulate the pH of endosomal or lysosomal microenvironments. The release profiles are shown in Figure. 5 (top). All the release profiles included two components: a rapid initial burst release and a slow release phase, as reported in other publications.<sup>31,32</sup> The rapid initial release might be attributed to following two reasons. One was the desorption of curcumin adsorbed on the micelle surfaces. The other was the fast diffusion of curcumin which was

located in the corona and the cores which is closely to the interface between the core and shell of the micelles.<sup>6,33</sup> In the following time, the release rates of curcumin from the micelles slowed down.

Obviously, the release rates of curcumin were remarkably influenced by the micelle's copolymer architecture and composition. At pH 7.4, 50% curcumin release from the drug-loaded L-PCL<sub>20</sub>-PEDA<sub>15</sub>SB<sub>5</sub> micelles took about 60 h, while the accumulative drug release for drug-loaded L-PCL<sub>20</sub>-PDEA<sub>10</sub>SB<sub>10</sub> micelles and 4s-PCL<sub>20</sub>-PDEA<sub>15</sub>SB<sub>5</sub> micelles was over 80% during the same time. This difference can be attributed to their different crystallinity. Highly crystalline linear copolymer can form highly packed crystals in micellar cores, which prevents drug release.<sup>6</sup> Just as indicated in Table 2, as sulfobetaine content and arm number increase, the degree of crystallization of the copolymer decrease. Consequently, with lower degree of crystallization the cores formed by PCL tend to be loose, which facilitates drug release from the micelles.

Moreover, the release rates of curcumin from the micelles were clearly influenced by pH values. The drug-loaded micelles of L-PCL<sub>20</sub>PDEA<sub>15</sub>SB<sub>5</sub> and 4s-PCL<sub>20</sub>PDEA<sub>15</sub>SB<sub>5</sub> exhibited faster drug release at lower pH than 7.4, while drug release rates from drug-loaded L-PCL<sub>20</sub>-PDEA<sub>10</sub>SB<sub>10</sub> micelles were almost same at both pH. The reason is, the micelles containing PDEA can be protonated at the pH lower than its pKa and the protonation of PDEA at low pH will increase the hydrophilicity of micellar shells, which result in expansion of shells, just as proved by the results of SEM (Figure 4). Ascribed to protonation of amine groups from DEA groups, the micelles expand and even break into smaller ones, resulting in drug release acceleration<sup>15</sup>. However, for L-PCL<sub>20</sub>PDEA<sub>10</sub>SB<sub>10</sub> micelles, there are less DEA groups and more sulfobetaine groups than in L-PCL<sub>20</sub>PDEA<sub>15</sub>SB<sub>5</sub> and 4s-PCL<sub>20</sub>PDEA<sub>15</sub>SB<sub>5</sub>. Thus, the effect of DEA protonation on micelle expansion at pH 5.0 is smaller. On the other hand, more sulfobetaine groups make L-PCL<sub>20</sub>PDEA<sub>10</sub>SB<sub>10</sub> be very hydrophilic (Figure 2) and its micelles own loose shells. In this case, L-PCL<sub>20</sub>PDEA<sub>10</sub>SB<sub>10</sub> micelles release curcumin with quite speed at pH 7.4. Consequently, the difference of the release rates of curcumin from the micelles is not obvious between different pH.

The drug release from a polymer matrix is a very complicated process. The mechanisms of drug release include pure diffusion, erosion control and their combination, which are affected by several factors such as polymer composition, molecular weight, hydrophilicity, crystallinity, degradation rate, micelle size, porosity and surface character<sup>34</sup>. To further understand the drug-release process of the copolymer micelles at pH 5.0 and pH 7.4, the release data were fitted to the following semi-empirical equation proposed by Ritger and Peppas:<sup>35,36</sup>

$$\frac{M_t}{M_\infty} = kt^n$$

Where,  $M_t$  and  $M_\infty$  are the absolute cumulative amounts of drug released at time  $t$  and infinite time, respectively,  $k$  is the release rate constant, and  $n$  is the diffusion exponent

indicating mechanism of drug release. For the drug release system of diffusion-erosion control with spherical particles, the value of  $n$  equals to 0.43, indicating diffusion-controlled drug release;  $0.43 < n < 0.85$  indicating the superposition of diffusion and swelling controlled drug release, which is usually called anomalous release; and  $n$  is equal to 0.85, indicating swelling-controlled drug release.

**Figure 5.** In vitro drug release of drug-loaded micelles of different micelles at pH = 7.4 and pH = 5.0 and plots of  $\log(M_t/M_\infty)$  against  $\log t$  for curcumin release from curcumin-loaded micelles at pH 7.4 and pH 5.0

The fitting curves of release data for the curcumin-loaded micelles were shown in Figure 5 (bottom) and the fitting data were summarized in Table 3. Fitting linearity at each stage was in accordance with the experimental data, indicating that the equation is applicable to the present systems. The results also show that the drug release behavior for these micelles were much different.

For L-PCL<sub>20</sub>PDEA<sub>15</sub>SB<sub>5</sub>/CUR micelles, the drug release showed three stages at both pH. At pH 7.4, it showed anomalous release during the first hour, and Fickian diffusion controlled drug release in the following two stage. In the beginning, as the micelle solution was transferred from the storing condition (4 °C) to the releasing condition (37 °C), increasing temperature will make the micelle swell to form superposition of diffusion and swelling controlled drug release (anomalous release). After that, the drug was released just by diffusion. At pH 5.0, the drug release after one hour was similar to that at pH 7.4, however, swelling-controlled drug release was found in the first stage. It was attributed to rapid protonation of DEA group after the micelle solution was transferred to an acidic condition. Protonation of DEA groups resulted in expansion of micelles. Just as shown in Figure. 5, it would release the drug which was attached onto the shell or located at the intermediate between shell and core. Moreover, there was some drug molecules associated with hydrophobic PDEA block. Protonation of DEA groups also made them to release rapidly. As a result, the drug release was mainly controlled by swelling in this period. Similarly, L-PCL<sub>20</sub>PDEA<sub>10</sub>SB<sub>10</sub>/CUR micelles at beginning stage displayed swelling-controlled release. Although the other part of the drug release curves at both pH were much approached, significant difference in release mechanism appeared only in the first drug release stage.

4s-PCL<sub>20</sub>PDEA<sub>15</sub>SB<sub>5</sub>/CUR micelles presented very different situation. There were only two drug release stages, that is, the first swelling-controlled release was not be observed at both pH. We suppose that this may be attributed to the lower capability of crystallinity for PCL segments in the four-armed copolymer, compared with linear copolymer L-PCL<sub>20</sub>PDEA<sub>15</sub>SB<sub>5</sub> (Table 2). The low crystallinity of PCL segments increased interaction between PDEA segments and PCL segments in micellar core formed by four-armed PCL, then, the time for the swelling process and protonation of DEA group was prolonged a lot. As a result, an overlapping

anomalous release process replaced two stage, controlled by swelling or diffusion separately.

### In vitro cytotoxicity

In vitro cytotoxicity of these micelles containing sulfobetaines was evaluated via MTT with LO2 cells. The results were summarized in Figure 6. L-PCL<sub>20</sub>PDEA<sub>10</sub>SB<sub>10</sub> and 4s-PCL<sub>20</sub>PDEA<sub>15</sub>SB<sub>5</sub> showed no significant toxicity to LO2 cells in 24h or 72h incubation, while L-PCL<sub>20</sub>PDEA<sub>15</sub>SB<sub>5</sub> showed slight cellular toxicity at medium concentration and significant toxicity at high concentration. The cell toxicity of PDEA-based copolymers is from DEA groups which can be protonated.<sup>37</sup> L-PCL<sub>20</sub>PDEA<sub>15</sub>SB<sub>5</sub> showed higher toxicity than L-PCL<sub>20</sub>PDEA<sub>10</sub>SB<sub>10</sub>, because of higher DEA content. Interestingly, even though L-PCL<sub>20</sub>PDEA<sub>15</sub>SB<sub>5</sub> and 4s-PCL<sub>20</sub>PDEA<sub>15</sub>SB<sub>5</sub> were same in constitution, the four-armed copolymer showed much less toxicity.

**Figure 6.** In vitro toxicity of the copolymer micelles to LO2 cells after 24 h (left) and 72 h (right) incubation at concentration of 5, 10, 30 mg mL<sup>-1</sup>

### Pharmacokinetics study

Based on the results of drug release and cytotoxicity in vitro, 4s-PCL<sub>20</sub>PDEA<sub>15</sub>SB<sub>5</sub> micelles were selected as carriers for curcumin in pharmacokinetics study. As shown in Figure 7. the CUR-loaded micelles significantly increased the retention time of curcumin in blood, while the free curcumin for CUR solution was quickly removed from the circulating system. After 1 h administration, the free curcumin of CUR solution in blood was less than 1000 ng/mL, while the curcumin of CUR-loaded micelles was approximate 5000 ng/mL, which was 5-fold in comparison with the former. To further analyse the drug-plasma profiles, the pharmacokinetic parameters, such as biological half-life ( $t_{1/2\alpha}$ ), area under the drug concentration-time curve values ( $AUC_{(0-\infty)}$ ), mean residence time ( $MRT_{(0-\infty)}$ ), and total clearance ( $CL/z$ ), were calculated by fitting the blood drug pharmaceutical concentrations to a two-compartment model using DAS2.1.1 software, and were summarized in insert Table. The clearance half-life  $t_{1/2\alpha}$  of CUR-loaded micelles was longer than that of CUR solution,  $t_{1/2\alpha}$  was 0.189 h and 0.133 h for CUR-loaded micelles and CUR solution, respectively. Meanwhile,  $AUC_{(0-\infty)}$  increased from 7832  $\mu\text{g/L}\cdot\text{h}$  to 16233  $\mu\text{g/L}\cdot\text{h}$  and  $C_{\text{max}}$  promoted from 3696  $\mu\text{g/L}$  to 11604  $\mu\text{g/L}$  for the CUR solution and the CUR-loaded micelles. In other word,  $AUC_{(0-\infty)}$  and  $C_{\text{max}}$  of the curcumin-loaded micelles enhanced around 2.07 fold and 3.14 fold, respectively, compared to the CUR solution. Whereas, CUR-loaded micelles also decreased  $CL/z$  compared to CUR solution. The results indicated that the pH sensitive micelles of star-shaped copolymer containing sulfobetaines obviously improved curcumin bioavailability in SD rats.

**Figure 7.** The profiles of concentration of curcumin in plasma versus time after intravenous injection of curcumin solution and curcumin micelles

## Biodistribution

The tissue distribution of CUR-loaded micelles and CUR solution after intravenous administration was compared in mice. Figure 8 demonstrated the distribution into the major organs and tumor tissue of breast carcinoma bearing BALB/c mice. The curcumin in tumor tissue for CUR-loaded micelles was distinct higher than that of CUR solution at 6 h post-injection, was 2.5-fold to latter. It's also significantly noted that the curcumin of CUR-loaded micelles in tumor tissue was substantially higher than that in other organ tissues except kidney, but this phenomenon did not exist in CUR solution group, suggesting the selective retention of 4s-PCL<sub>20</sub>PDEA<sub>15</sub>SB<sub>5</sub> micelles in tumor tissue. The preferential tumor uptake of the micelles was likely due to the prolonged circulation and the EPR effect. There were no evident distinction of curcumin content between CUR solution and CUR-loaded micelles in normal organs, indicating that curcumin-loaded micelles enhanced drug bioavailability without obviously increased the entered drug amount into the major organs. As a result, the extension of drug half-life time would not bring more harm to the major organs. As to higher curcumin content in kidney than other organs for both CUR-loaded micelles and CUR solution, it might be because curcumin was mainly excreted out of mice by kidney.

**Figure 8.** Biodistribution data of free CUR solutions and CUR-loaded micelles given intravenously at a dose of 10 mg/kg in mice for 6h.

## Histopathology

In order to explore whether CUR-loaded micelles bring acute harm to major organs of the breast carcinoma bearing BALB/c mice, parts of the organs harvested in the biodistribution experiment were sliced for pathological observation.<sup>38</sup> The results of histopathology for the major organs showed that there were no histomorphology change in heart, spleen, brain and kidney for control group, CUR solution and CUR-loaded micelles, meanwhile, the tissue section images of lung, liver and tumor shown in Figure 9, had significantly histomorphology change. In comparison with the lung tissue section of control group, the perivascular and interstitial inflammatory infiltrates with mildly thickened alveolar walls were seen for CUR solution, while that phenomenon was not obvious for the lung tissue section of BALB/c mice injected with CUR-loaded micelles.

**Figure 9.** Hematoxylin-eosin staining after 6h of CUR given intravenously at a dose of 10 mg/kg in mice.

In liver tissue section, hepatocyte focal edema presented surrounding the portal area in control group, and part of hepatic cells appeared bleeding phenomenon in CUR solution group, while hepato edema disease significantly reduced in BALB/c mice injected with CUR-loaded group.

The tumor tissue section of control group displayed that the tumor cells closely arranged, the nuclear/cytoplasmic ratios increased, and the boundary between parenchyma and

intercellular substance became unclear. The irregularity of cellular morphology, increase of pathological karyokinesis phase, new vessels in intercellular substance with uncompleted basement membrane and few thrombus caused by invasion vessel of tumor cells were also observed. However, for mice injected with CUR solution, the tumor tissue section showed that the arrangement of tumor tissue cells was loose, multiple patchy necrosis appeared in tumor foci and the centre gap of tumor tissue increased. Moreover, the light transmittance of tumor tissue section improved. The protein-like material and cell debris presented in the section. A portion of vascular contours was destructed, and mass of neutrophile granulocyte in partial region infiltrated. All the phenomena implied that tumor tissue necrosis started to happen. As for mice injected with CUR-loaded micelles, all the symptoms of tumor necrosis emerged slightly serious in tumor tissue section.

In conclusion, no histomorphology changes caused by CUR solution and CUR-loaded micelles in main substantive organs such as heart, spleen, brain and kidney were observed. CUR-loaded micelles improve the curcumin influence on lung and liver and have potential to tumor treatment.

## Conclusion

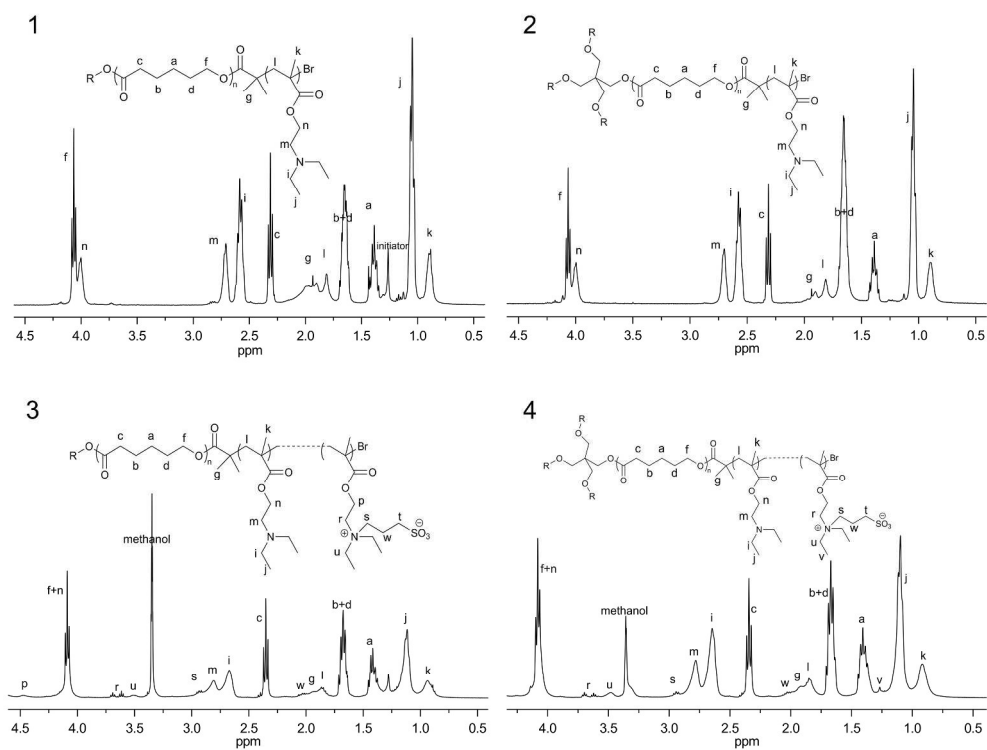
Three copolymers composed of PCL, DEA groups and sulfobetaine groups with linear and four-armed star shape were prepared via a combination of ROP, ATRP and post sulfonation. The copolymers thermal properties, hydrophilicity, micelle properties, pH sensitivity and drug releasing performance were effected by their composition/structure. The micelles of the star-shaped copolymer displayed lower cell toxicity than those of the linear copolymer with the same composition. The drug release rate of the curcumin-loaded micelles was related to sulfobetaine content and the architecture of the copolymers. The curcumin-loaded micelles prolonged the retention time of curcumin in blood circulation and accumulated more in tumor site than the free curcumin in breast carcinoma bearing mice, and could reduce curcumin damage to liver and lung. The pH sensitive micelles of star-shaped copolymer containing sulfobetaines with suitable composition displayed promising application as carriers for hydrophobic drugs.

## Acknowledgements

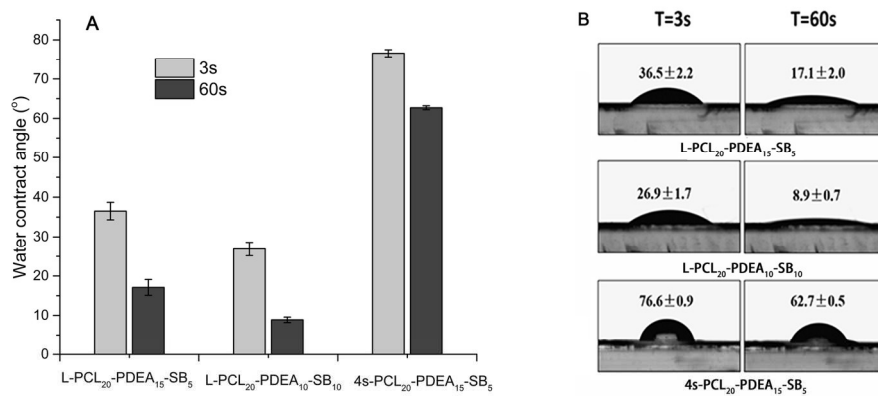
This work was supported by the National Natural Science Foundation of China (no. 51473099 and 51273125). We would also like to appreciate our laboratory members for the generous help, and gratefully acknowledge the Analytical and Testing Center at Sichuan University for test

## Notes and references

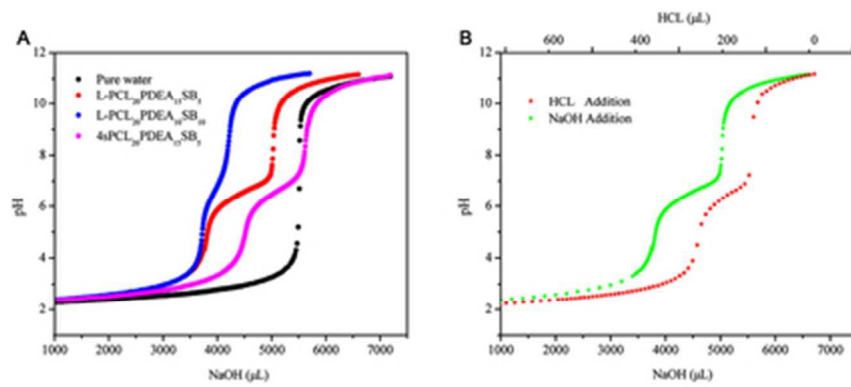
1. H. M. Aliabadi, S. Elhasi, A. Mahmud, R. Gulamhusein, P. Mahdipoor and A. Lavasanifar, *INTERNATIONAL JOURNAL OF PHARMACEUTICS*, 2007, **329**, 158-165.
2. R. H. D. F. Katrin Knop, *ANGEWANDTE CHEMIE-INTERNATIONAL EDITION*, 2010, 6288-6308.
3. S. M. D. B. Julien Nicolas, *chemical society reviews*, 2012, 1147-1235.
4. H. Tian, Z. Tang, X. Zhuang, X. Chen and X. Jing, *Progress in Polymer Science*, 2012, **37**, 237-280.
5. M. Zhang, W. Shen, Q. Xiong, H. Wang, Z. Zhou, W. Chen and Q. Zhang, *RSC Adv.*, 2015, **5**, 28133-28140.
6. J. Cao, A. Lu, C. Li, M. Cai, Y. Chen, S. Li and X. Luo, *Colloids and Surfaces B: Biointerfaces*, 2013, **112**, 35-41.
7. S. Khoei and M. T. Hossainzadeh, *Colloids and Surfaces B: Biointerfaces*, 2010, **75**, 133-140.
8. J. Liu, Y. Huang, A. Kumar, A. Tan, S. Jin, A. Mozhi and X. Liang, *Biotechnology Advances*, 2014, **32**, 693-710.
9. M. Cai, K. Zhu, Y. Qiu, X. Liu, Y. Chen and X. Luo, *Colloids and Surfaces B: Biointerfaces*, 2014, **116**, 424-431.
10. B. Romberg, W. E. Hennink and G. Storm, *Pharmaceutical Research*, 2008, **25**, 55-71.
11. E. A. Van Kirk And William J. Murdoch, *AIChE Journal*, 2008.
12. S. Lin, F. Du, Y. Wang, S. Ji, D. Liang, L. Yu and Z. Li, *Biomacromolecules*, 2008, **9**, 109-115.
13. J. Cao, S. Zhai, C. Li, B. He, Y. Lai, Y. Chen, X. Luo and Z. Gu, *Journal of Biomedical Nanotechnology*, 2013, **9**, 1847-1861.
14. N. Murthy, J. Campbell, N. Fausto, A. S. Hoffman and P. S. Stayton, *Bioconjugate Chemistry*, 2003, **14**, 412-419.
15. S. Zhai, Y. Ma, Y. Chen, D. Li, J. Cao, Y. Liu, M. Cai, X. Xie, Y. Chen and X. Luo, *Polym. Chem.*, 2014, **5**, 1285-1297.
16. J. Fan, F. Zeng, S. Wu and X. Wang, *Biomacromolecules*, 2012, **13**, 4126-4137.
17. Q. Jin, Y. Chen, Y. Wang and J. Ji, *Colloids and Surfaces B: Biointerfaces*, 2014, **124**, 80-86.
18. W. Kuo, M. Wang, H. Chien, T. Wei, C. Lee and W. Tsai, *Biomacromolecules*, 2011, **12**, 4348-4356.
19. J. A. Pedro, J. R. Mora, M. Silva, H. D. Fiedler, C. A. Bunton and F. Nome, *Langmuir*, 2012, **28**, 17623-17631.
20. C. Shen and J. Lin, *Colloids and Surfaces B: Biointerfaces*, 2013, **101**, 376-383.
21. J. Cao, K. Xiu, K. Zhu, Y. Chen and X. Luo, *Journal of Biomedical Materials Research Part A*, 2012.
22. V. A. Sethuraman, K. Na and Y. H. Bae, *Biomacromolecules*, 2006, **7**, 64-70.
23. J. Cao, X. Xie, A. Lu, B. He, Y. Chen, Z. Gu and X. Luo, *Biomaterials*, 2014, **35**, 4517-4524.
24. Z. Yang, J. Liu, Z. Huang and W. Shi, *European Polymer Journal*, 2007, **43**, 2298-2307.
25. C. Mohanty, S. Acharya, A. K. Mohanty, F. Dilnawaz and S. K. Sahoo, *Nanomedicine*, 2010, **5**, 433-449.
26. K. Kataoka, A. Harada and Y. Nagasaki, *Adv Drug Deliv Rev*, 2001, **47**, 113-131.
27. M. Gou, K. Men, H. Shi, M. Xiang, J. Zhang, J. Song, J. Long, Y. Wan, F. Luo, X. Zhao and Z. Qian, *Nanoscale*, 2011, **3**, 1558-1567.
28. L. Huang, M. Cai, X. Xie, Y. Chen and X. Luo, *Journal of Biomaterials Science, Polymer Edition*, 2014, **25**, 1407-1424.
29. A. Sahu, N. Kasoju, P. Goswami and U. Bora, *Journal of Biomaterials Applications*, 2011, **25**, 619-639.
30. H. A. M. O. Ma Z, *journal of biomedical materials research part a*, 2007.
31. J. C. H. Y. So Yeon Kim, *Journal of Controlled Release*, 2000.
32. C. Li, W. Beilei, L. Yanjun, C. Jun, Tingting, J. Feng, C. Yuanwei and X. Luo, *journal of biomaterials science-polymer edition*, 2012.
33. J. Cao, F. Cheng, H. Cao, A. Lu, M. Cai, Y. Chen, B. He, Z. Gu and X. Luo, *Colloids and Surfaces B: Biointerfaces*, 2015, **125**, 213-221.
34. J. Albuerne, L. Márquez, A. J. Müller, J. M. Raquez, P. Degée, P. Dubois, V. Castelletto and I. W. Hamley, *Macromolecules*, 2003, **36**, 1633-1644.
35. P. L. Ritger, N. A. Peppas, P. L. Ritger and N. A. Peppas, *Journal of Controlled Release*, 1987, **5**, 37-42.
36. P. L. Ritger and N. A. Peppas, *Journal of Controlled Release*, 1987, **5**, 23-36.
37. J. P. Salvage, S. F. Rose, G. J. Phillips, G. W. Hanlon, A. W. Lloyd, I. Y. Ma, S. P. Armes, N. C. Billingham and A. L. Lewis, *Journal of Controlled Release*, 2005, **104**, 259-270.
38. A. Gülçubuk, K. Sönmez, A. Gürel, K. Altunatmaz, N. Gürler, S. Aydın, L. Öksüz, H. Uzun and Ö. Güzel, *Pancreatology*, 2005, **5**, 345-353.



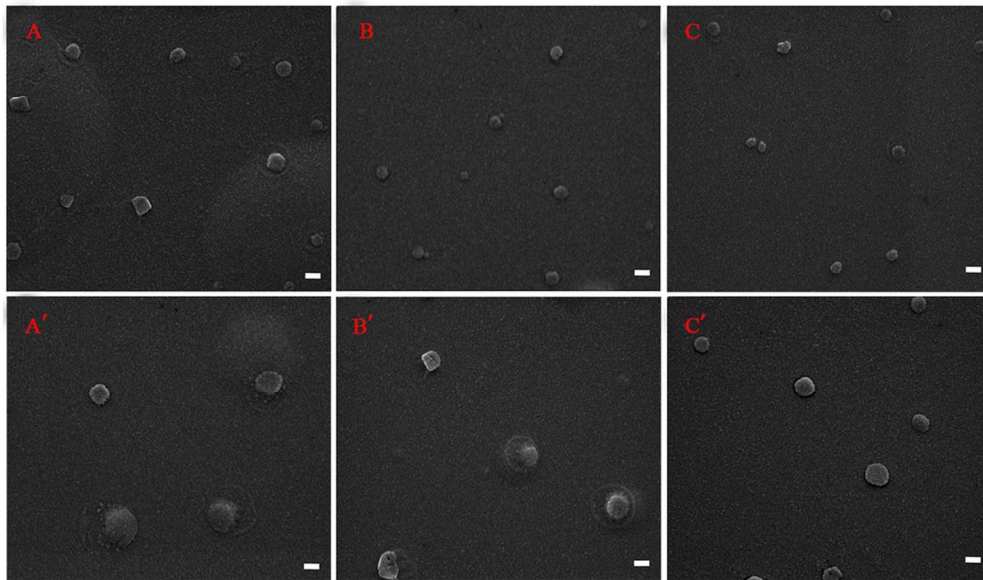
132x102mm (600 x 600 DPI)



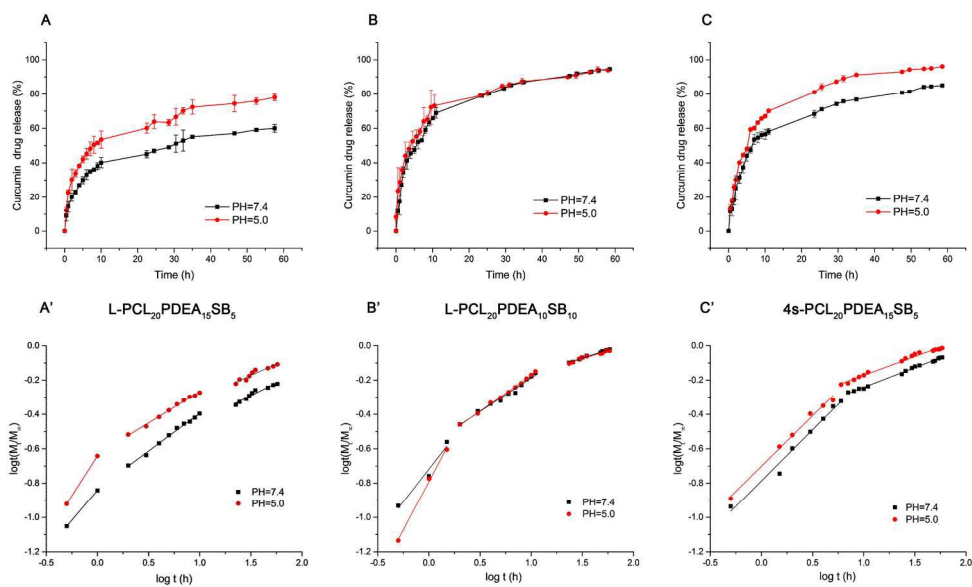
79x37mm (600 x 600 DPI)



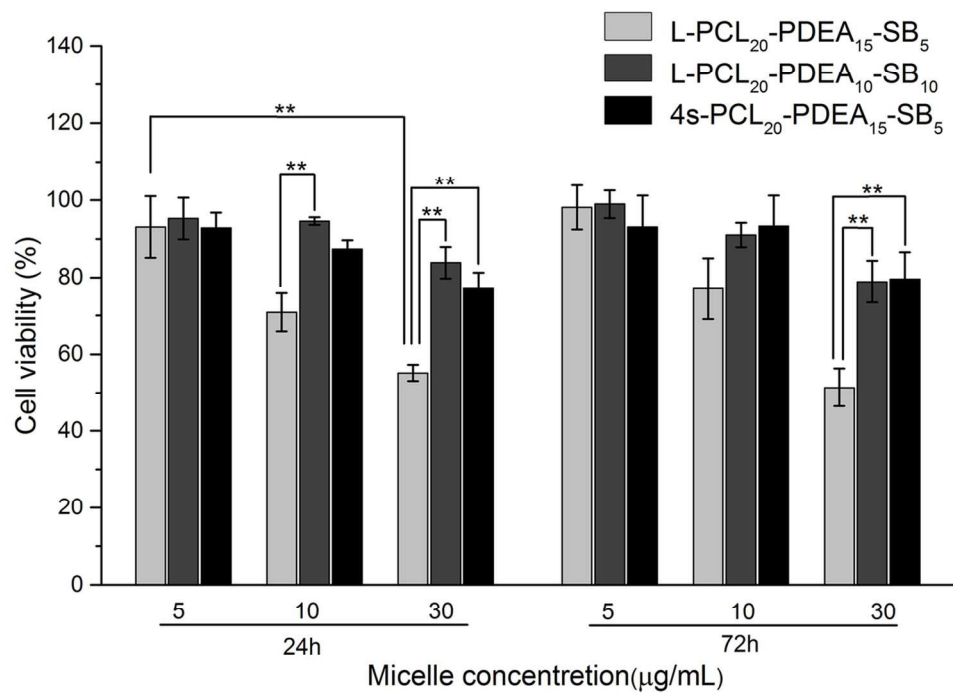
37x17mm (300 x 300 DPI)



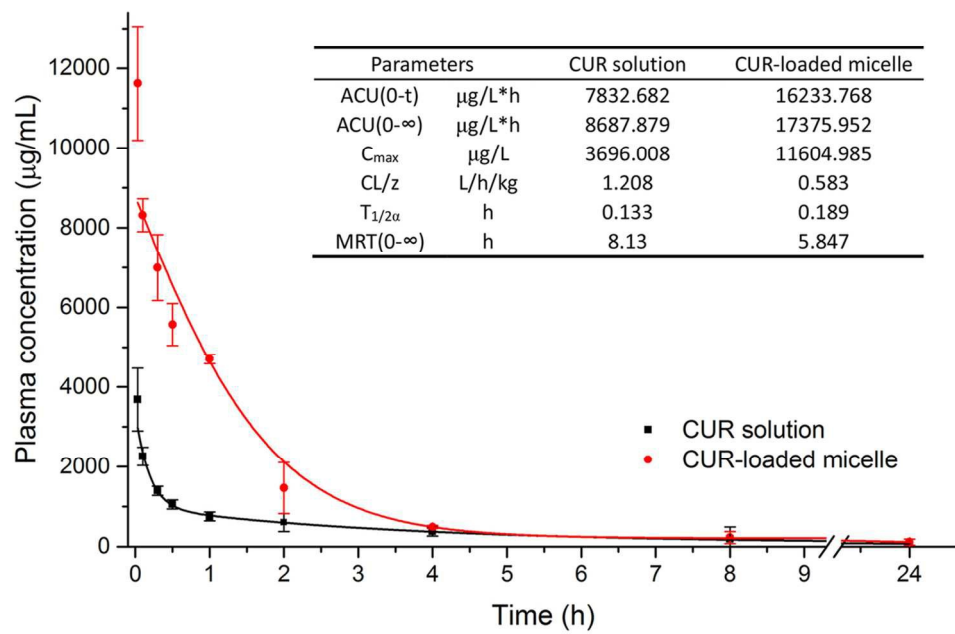
48x28mm (600 x 600 DPI)



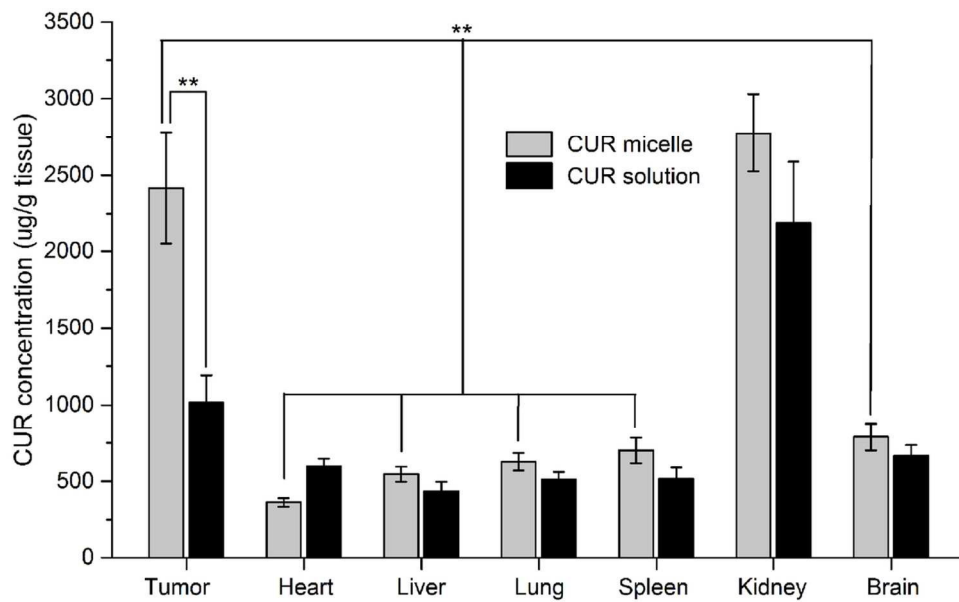
104x63mm (600 x 600 DPI)



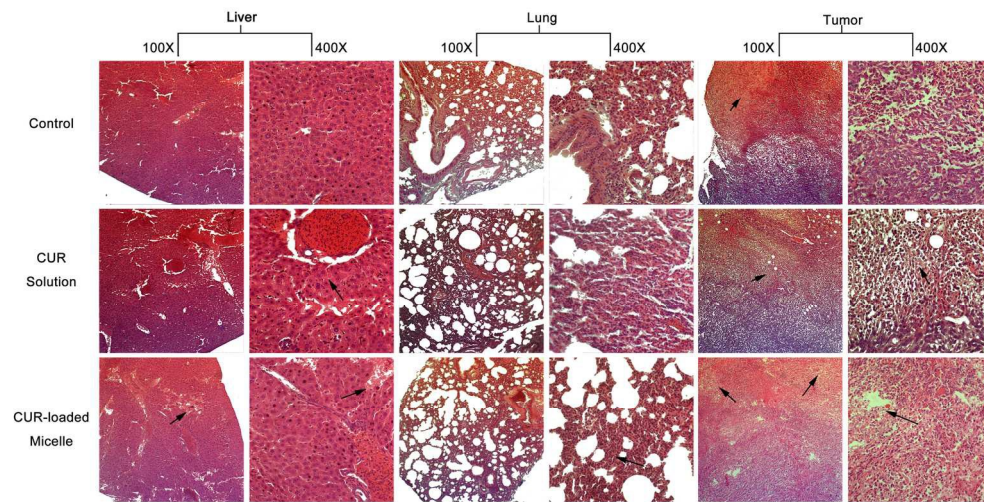
62x46mm (600 x 600 DPI)



59x43mm (600 x 600 DPI)



56x38mm (600 x 600 DPI)



87x45mm (600 x 600 DPI)

Copolymer	$M_n^a$	$M_w^b$	$M_n^b$	PDI <sup>b</sup>	[SBMA] <sup>c</sup>	[SBMA] <sup>d</sup>	$X_c(\%)^f$
L-PCL <sub>20</sub> PDEA <sub>20</sub>	6.5K	8.0K	5.5K	1.467	- <sup>e</sup>	- <sup>e</sup>	27.09
4sPCL <sub>20</sub> PDEA <sub>20</sub>	23.2K	22.4K	10.4K	2.160	- <sup>e</sup>	- <sup>e</sup>	13.53
L-PCL <sub>20</sub> PDEA <sub>15</sub> SB <sub>5</sub>	7.0K	- <sup>e</sup>	- <sup>e</sup>	- <sup>e</sup>	3	5	20.73
L-PCL <sub>20</sub> PDEA <sub>10</sub> SB <sub>10</sub>	8.0K	- <sup>e</sup>	- <sup>e</sup>	- <sup>e</sup>	12	9	13.27
4sPCL <sub>20</sub> PDEA <sub>15</sub> SB <sub>5</sub>	25.7K	- <sup>e</sup>	- <sup>e</sup>	- <sup>e</sup>	5	5	5.24

**Table 1.** Composition and crystallinity data for L/4sPCL-b-PDEA and the resulting L/sPCL-b-PDEAS copolymers

<sup>a</sup> Molecular weight calculated from <sup>1</sup>H NMR spectra;

<sup>b</sup> Molecular weight and PDI determined by GPC result;

<sup>c</sup> Unit number of sulfobetaine group, calculated from <sup>1</sup>H NMR spectra;

<sup>d</sup> Unit number of sulfobetaine group, calculated from element analysis;

<sup>e</sup> "-" means that the item does not exist or could not be measured for the sample.

<sup>f</sup> Degree of crystallinity determined by DSC result.

**Table 2.** Preparation and characterization of the blank micelles and drug-load micelles

Sample	CMC (mg/L)	Diameter (nm)	PDI	Zeta-potential (mV)	DLC (%)	DLE (%)
L-PCL <sub>20</sub> PDEA <sub>15</sub> SB <sub>5</sub> <sup>a</sup>	1.82	63.3±0.3	0.155±0.010	52.7±1.0	-c	-c
L-PCL <sub>20</sub> PDEA <sub>10</sub> SB <sub>10</sub> <sup>a</sup>	1.88	70.4±0.1	0.214±0.006	41.6±0.8	-c	-c
4sPCL <sub>20</sub> PDEA <sub>15</sub> SB <sub>5</sub> <sup>a</sup>	0.72	69.3±1.1	0.286±0.012	51.8±2.0	-c	-c
L-PCL <sub>20</sub> PDEA <sub>15</sub> SB <sub>5</sub> /CUR <sup>b</sup>	- <sup>c</sup>	78.6±0.2	0.222±0.005	58.8±3.0	11.22±0.73	56.1±3.7
L-PCL <sub>20</sub> PDEA <sub>10</sub> SB <sub>10</sub> /CUR <sup>b</sup>	- <sup>c</sup>	109.9±1.1	0.394±0.006	46.7±1.5	12.87±0.52	64.5±2.6
4sPCL <sub>20</sub> PDEA <sub>15</sub> SB <sub>5</sub> /CUR <sup>b</sup>	- <sup>c</sup>	103.0±5.0	0.391±0.050	56.6±5.0	10.41±0.61	52.0±3.5

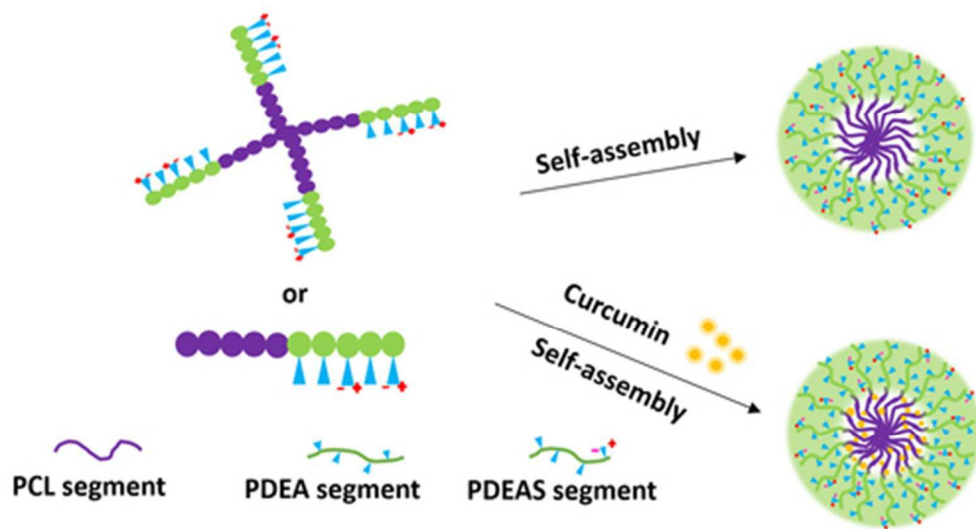
<sup>a</sup> Blank micelles were prepared with ultra-purified water and the final concentration of the micelle is 1 mg/ml;

<sup>b</sup> Drug loaded micelles were prepared with ultra-purified water and the mass ratio of the copolymer and curcumin is about 5.

<sup>c</sup> “-” means that the item does not exist or could not be measured for the sample.

**Table 3.** Release exponent (n), rate constant (k) and correlation coefficient ( $R^2$ ) for the drug-loaded micelles of the different copolymers

Samples	Time interval	pH=7.4			pH=5.0		
		n	k	$R^2$	n	k	$R^2$
L-PCL <sub>20</sub> PDEA <sub>15</sub> SB <sub>5</sub> /CUR	0-1	0.694	0.075	1.000	0.928	0.192	1.000
	1-12	0.440	0.078	0.997	0.368	0.197	0.997
	23-60	0.298	0.132	0.975	0.263	0.247	0.959
SL-PCL <sub>20</sub> PDEA <sub>10</sub> SB <sub>10</sub> /CUR	1-1.5	0.756	0.142	0.984	1.124	0.102	0.998
	2-12	0.394	0.234	0.992	0.413	0.228	0.999
	23-60	0.194	0.438	0.994	0.181	0.458	0.986
4sPCL <sub>20</sub> PDEA <sub>15</sub> SB <sub>5</sub> /CUR	0-3	0.592	0.103	0.992	0.589	0.152	0.991
	4-60	0.226	0.329	0.998	0.218	0.407	0.993



43x23mm (300 x 300 DPI)